Dalton
Transactions

Cite this: *Dalton Trans.*, 2011, **40**, 2067

www.rsc.org/dalton

PAPER

Dimerization of pentanuclear clusters $[Fe_3Q(AsMe)(CO)_9]$ (Q = Se, Te) as a conversion pathway to novel cubane-like aggregates†‡

Nikolay A. Pushkarevsky,*[a] Sergey N. Konchenko,[a] Manfred Zabel,[b] Michael Bodensteiner[b] and Manfred Scheer*[b]

Received 15th November 2010, Accepted 4th January 2011
DOI: 10.1039/c0dt01587c

The first examples of carbonyl heterocubane-type clusters, $[Fe_4(\mu_3\text{-}Q)_2(\mu_3\text{-}AsMe)_2(CO)_{12}]$ (**2**, Q = Se (**a**), Te (**b**)), which simultaneously contain elements of group 15 and 16, were obtained by thermolysis of $[Fe_3(\mu_3\text{-}Q)(\mu_3\text{-}AsMe)(CO)_9]$ (**1**) in acetonitrile. The clusters **2** possess a cubic $Fe_4Q_2As_2$ core with alternating Fe and Q/As atoms. The coordination environment of the Fe atoms is close to octahedral, and those of Q or As atoms are tetrahedral, which determines the distorted cubic cluster core geometry. The second main products of thermolysis are the clusters $[Fe_6(\mu_3\text{-}Q)(\mu_4\text{-}Q)(\mu_4\text{-}AsMe)_2(CO)_{12}]$ (**3a,b**), whose core contains double the elemental composition of the initial cluster **1**. In the case of the Se-containing cluster two other minor products $[Fe_4(\mu_4\text{-}Se)(\mu_4\text{-}SeAsMe)(CO)_{12}]$ (**4**) and $[Fe_3(\mu_3\text{-}AsMe)_2(CO)_9]$ (**5**) are formed. Based on the structures and properties of the products, a reaction route for the conversion of **1** into **2** is proposed, which includes the associative formation of the clusters **3** as intermediates, unlike the dissociative pathways previously known for the transformations of similar clusters of the type $[Fe_3Q_2(CO)_9]$.

Introduction

Heterocubane-type iron clusters with a Fe_4Q_4 core (Q = S, Se, Te) are classes of compounds of increasing research interest. For instance the sulfur-containing clusters are extensively studied as models of ferredoxin cofactors.[1] Depending on the supporting ligands (SR, Cp^x, CO, NO, halogen), the cluster core possesses different numbers of Fe–Fe bonds and the metals often possess different oxidation states.[2–4] Consequently, the clusters are interesting in respect to their redox properties and reactivity. In contrast the analogous clusters with the core $M_4(ER)_4$, containing group 15 element vertices ER in place of chalcogen atoms, are much less common, and only a few examples with nitrogen,[5] arsenic,[6] or antimony are known.[7] Interestingly, the heterocubane clusters, containing both group 16 and 15 element vertices, are not known at all, although compounds with different terminal ligands in one molecule, as well as those with different metal vertices, are common.[8]

Concerning carbonyl clusters, the chalcogen-containing species $[Fe_4Q_4(CO)_{12}]$ can be synthesized either by dimerization of binuclear iron species $[Fe_2Q_2(CO)_6]$ (Q = S, Te),[4] or by substitution of NO ligands for CO in the clusters $[Fe_4Q_4(NO)_4]$ (Q = S, Se).[3] To date, heavy group 15 element cubane clusters $[Fe_4(AsMe)_4(CO)_{12}]$[9] and $[Fe_4(SbFeCp(CO)_2)_4(CO)_{12}]$[7] are known, which have been obtained as the result of thermolysis of iron carbonyl complexes with As- or Sb-based ligands. We have developed convenient methods for synthesis of tri-iron clusters $[Fe_3(\mu_3\text{-}Q)(\mu_3\text{-}ER)(CO)_9]$ with both group 15 (E = As, Sb, Bi) and group 16 (Q = Se, Te) element vertices.[10,11] Those clusters are isoelectronic with their chalcogen-only analogs, revealing the same core geometry and quite similar reactivity towards metal vertex addition and substitution.[12–15] It was of further interest to check whether the mixed group 15/16 element clusters can be used for the synthesis of heterocubane clusters with different non-metal vertices. Indeed, the novel clusters with the core $[Fe_4Q_2As_2]$ were obtained by thermolysis of $[Fe_3Q(AsMe)(CO)_9]$ (**1**). Moreover, the second main products showing the unusual $[Fe_6Q_2As_2]$ decanuclear cluster core reveal a dimerization of the initial clusters **1**, which do not match the existing schemes of $[Fe_3Q_2]$ or $[Fe_3Q(ER)]$ cluster core transformations. Possible reaction pathways and the influence of the AsMe ligand on the reactivity of the cluster are discussed below.

Results and discussion

Synthesis

It is known from the work of Rauchfuss and co-workers[4] that the thermolysis of the pyramidal cluster $[Fe_3Te_2(CO)_9]$ in acetonitrile leads to its conversion into the corresponding cubane compound $[Fe_4Te_4(CO)_{12}]$. The used method includes heating in acetonitrile

---

[a] *Nikolaev Institute of Inorganic Chemistry, Siberian Division of RAS, Akad. Lavrentyeva str. 3, 630090, Novosibirsk, Russia. E-mail: nikolay@niic.nsc.ru*
[b] *Institut für Anorganische Chemie, Universität Regensburg, 93040, Regensburg, Germany. E-mail: manfred.scheer@chemie.uni-regensburg.de*

† CCDC reference numbers 802724–802731. For crystallographic data in CIF or other electronic format see DOI: 10.1039/c0dt01587c

‡ Dedicated to Prof. Peter Klüfers on the occasion of his 60th birthday.

in the presence of a high pressure of CO (136 bar). In the absence of CO the cluster [$Fe_2Te_2(CO)_6$] forms instead of the cubane cluster. Another simple method of generating the [$Fe_2QQ'(CO)_6$] (Q, Q′ = S, Se, Te in all combinations) species in solution, discovered by Rauchfuss and further developed by Mathur and co-workers,[16] is the reaction of the corresponding pyramidal clusters [$Fe_3QQ'(CO)_9$] with NaOMe in methanol. By studying the analogous pyramidal clusters [$Fe_3Q(AsMe)(CO)_9$] (Q = Se, Te) we have found to our surprise, that the same reactions applied do not lead to any conversion. Indeed, heating the chalcogen/AsMe-containing clusters **1** in acetonitrile under CO pressure with the conditions close to those mentioned in the literature[4] (136 bar CO, 80 °C, 3 days) did not result in any noticeable changes to the appearance of the reaction solutions. The starting clusters were the only species present in the solution in the autoclave (IR monitoring) and no decomposition was observed. Analogously, after the treatment of [$Fe_3Q(AsMe)(CO)_9$] with NaOMe in methanol and further acidification and extraction with hexane the starting clusters are almost quantitatively retrieved. This reaction behaviour is in contrast to the fact that the clusters [$Fe_3Q(AsMe)(CO)_9$] have the same square-pyramidal structure as the dichalcogenide analogs and similar chemical behaviour in the previously studied reactions have been observed, including addition and substitution of the metal vertex.[12–14]

Nevertheless, the clusters [$Fe_3Q(AsMe)(CO)_9$], being so stable under rather severe conditions, readily transform upon heating in acetonitrile at 70 °C (in a closed evacuated vessel) without any additional CO pressure. Most of the initial cluster reacts overnight, leaving about 20% of the unreacted starting compound (the quantities of individual products were determined after column chromatographic workup). The extractive workup with toluene leads to an intractable oily black residue (about 30% of the mass of the starting cluster), which is a multi-component mixture of compounds according to the NMR and IR spectra. This residue could be neither separated chromatographically, nor crystallized from common solvents, and remained uncharacterized. The soluble compounds could be separated by column chromatography with a hexane–toluene mixture as the eluent. There are two main bands: the first, brown in colour, contains a mixture of starting cluster and the cubane cluster **2** (Scheme 1), the second, dark grey fraction, contains the product **3**. For the reaction of Te-containing compound **1b** only the above mentioned bands were detected, while in the case of the Se-containing starting cluster **1a** several weakly colored bands were also detectable, two of which were collected. The brown-grey band, which appears after the main grey fraction, gives a few black crystals of **4** after concentration and subsequent cooling. However, the crystals did not redissolve in toluene. The second brownish band coming just after the first brown band, was shown to contain small amounts of cluster **5**.

Crystal structures and characterization

All products **2**, **4**, and **5** have been characterized by X-ray diffraction analysis. For compounds **3**, the crystal structure for Te-containing cluster **3b** was determined; the isostructural Se-containing analog **3a** was identified by IR, NMR, and mass spectroscopic data (see below).

Crystal structural data for **2–5** are summarized in Tables 1 and 2. While studying different conditions necessary for the cluster formation, two different crystal structures for compound **2a** and three for compound **2b** were obtained.

For **2a**, one crystal structure represents the pure cluster and the other one its solvate **2a**·CH_2Cl_2. Interestingly, while the solvate was obtained by layering of a solution of reaction products in CH_2Cl_2 with hexane at room temperature, the solvent-free crystals were formed from the pure CH_2Cl_2 solution of the compound mixture at lower temperatures (–25 °C).

For **2b**, there are two different solvent-free polymorphs: the one with orthorhombic cell parameters (**2b**^{o}) was obtained directly by cooling the acetonitrile reaction solution, and another one, with a monoclinic structure (**2b**^{m}) was grown during the crystallization of the toluene extract of the products from a toluene–hexane mixture. The third structure is a solvate **2b**·CH_2Cl_2, which readily crystallizes upon cooling the CH_2Cl_2 solution of the pure compound **2b**, separated by chromatography. This solvate is isostructural with **2a**·CH_2Cl_2. The structural parameters for the clusters **2a** and **2b** in different crystal systems are very similar, the relative differences of the corresponding bond lengths and angles in the cluster core do not exceed 1%. The molecular structures of **2a** and **2b** resemble a distorted cube with alternating metal and non-metal vertices (Fig. 1). The coordination environment of the Fe atoms is close to octahedral, and that of the As atoms close to tetrahedral (angle Fe–As–Fe ~102° (**2a**), ~104° (**2b**)). The Fe–Q–Fe angles are somewhat closer to 90°, and slightly differ for the cluster containing Se (~97°) and Te (~95°). The angles at the non-metal atoms are close to those at the corresponding As and Te atoms in the related cubane clusters: [$Fe_4(AsMe)_4(CO)_{12}$] (angles Fe–As–Fe 102.6(2)°),[6] [$Fe_4Q_4(CO)_{12}$] (Q = S: angles Fe–S–Fe 95.4–96.9(1)°; Q = Se: angles Fe–Se–Fe 95.4(1) and 96.7(1)°).[3] In all cases, the angles at the As atoms are noticeably larger than those

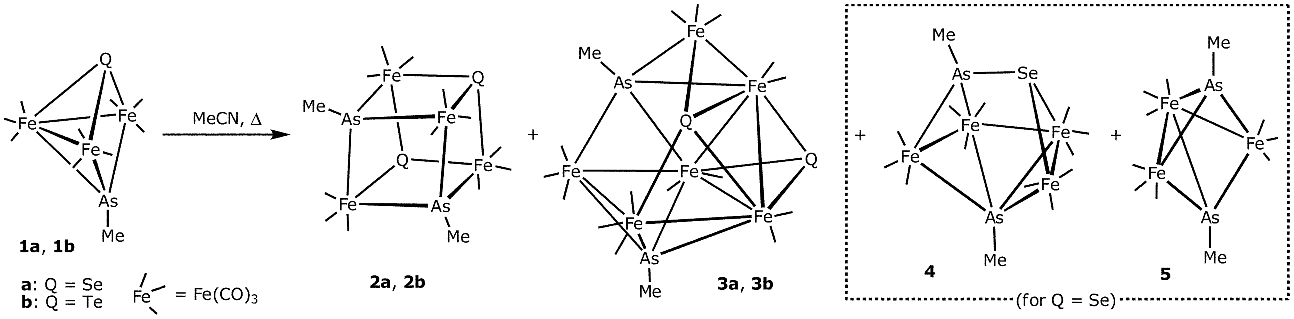

Scheme 1

Table 1 Crystallographic data for the structures of **2a**·$\mathrm{CH_2Cl_2}$ and **2b** (all modifications)

	2a·$\mathrm{CH_2Cl_2}$	**2b**·$\mathrm{CH_2Cl_2}$	**2b** (monoclinic)	**2b** (orthorhombic)
Empirical formula	$\mathrm{C_{15}H_8As_2Cl_2Fe_4O_{12}Se_2}$	$\mathrm{C_{15}H_8As_2Cl_2Fe_4O_{12}Te_2}$	$\mathrm{C_{14}H_6As_2Fe_4O_{12}Te_2}$	$\mathrm{C_{14}H_6As_2Fe_4O_{12}Te_2}$
Formula weight	982.27	1079.55	994.63	994.63
Temperature (K)	200(2)	123(1)	203(2)	203(2)
λ(Å)	0.56087 (Ag-Kα)	0.71073 (Mo-Kα)	0.56087 (Ag-Kα)	0.56087 (Ag-Kα)
Crystal system	Monoclinic	Monoclinic	Monoclinic	Orthorhombic
Space group	$P2_1/n$	$P2_1/n$	$P2_1/c$	$Ima2$
a (Å)	10.397(2)	10.2566(14)	13.021(3)	26.694(3)
b (Å)	17.966(4)	17.710(3)	9.977(2)	16.950(2)
c (Å)	15.416(3)	15.4128(17)	19.555(4)	11.046(2)
α (°)	90	90	90	90
β (°)	92.02(3)	92.092(14)	90.08(3)	90
γ (°)	90	90	90	90
V (Å^3)	2877.8(10)	2797.8(7)	2540.4(9)	4997.9(17)
Z	4	4	4	8
μ (mm^{-1})	3.686	6.669	3.739	3.801
D_{calc} (g cm^{-3})	2.267	2.563	2.601	2.644
F(000)	1 864	1995	1 840	3 680
Θ Range (°)	2.07–25.91	3.26–33.01	2.19–22.42	2.04–22.42
Index ranges	$-15 \le h \le 15$	$-14 \le h \le 14$	$-16 \le h \le 16$	$-35 \le h \le 35$
	$-27 \le k \le 27$	$-25 \le k \le 25$	$-13 \le k \le 11$	$-22 \le k \le 23$
	$-19 \le l \le 23$	$-22 \le l \le 22$	$-26 \le l \le 26$	$-14 \le l \le 14$
R_{int}	0.1064	0.0560	0.0424	0.0517
Reflections measured	24851	25291	15121	17892
Independent reflections	10 996	8653	6261	6323
Parameters	348	371	309	325
Goodness-of-fit on F^2	1.252	1.078	1.032	1.033
Final R_1, wR_2 ($I > 2\sigma(I)$) (all data)	0.0778, 0.1985	0.0359, 0.0761	0.0325, 0.0690	0.0330, 0.0761
	0.1395, 0.2399	0.0710, 0.0954	0.0490, 0.0744	0.0407, 0.0798
Largest difference peak and hole (e Å^{-3})	1.787	1.316	0.859	1.560
	−2.417	−1.195	−0.697	−1.020

Table 2 Crystallographic data for the structures of **2a**, **3b**, **4**, and **5**

	2a	**3b**·0.5$\mathrm{CH_2Cl_2}$	**4**	**5**
Empirical formula	$\mathrm{C_{14}H_6As_2Fe_4O_{12}Se_2}$	$\mathrm{C_{17.5}H_7As_2ClFe_6O_{15}Te_2}$	$\mathrm{C_{14}H_6As_2Fe_4O_{12}Se}$	$\mathrm{C_{11}H_6As_2Fe_3O_9}$
Formula weight	897.35	1232.82	818.39	599.54
Temperature (K)	123(2)	123(2)	123(1)	123(2)
λ(Å)	0.71073 (Mo-Kα)	0.71073 (Mo-Kα)	1.54178 (Cu-Kα)	0.71073 (Mo-Kα)
Crystal system	Monoclinic	Monoclinic	Triclinic	Orthorhombic
Space group	$P2_1/n$	$C2/c$	$P\bar{1}$	$Cmc2_1$
a (Å)	8.5776(2)	17.7104(4)	9.9663(4)	10.6982(4)
b (Å)	29.8122(4)	11.0072(2)	10.5051(4)	12.3724(4)
c (Å)	9.6766(2)	31.0735(6)	10.6381(5)	13.0665(4)
α (°)	90	90	85.208(4)	90
β (°)	107.589(2)	92.1845(18)	85.591(4)	90
γ (°)	90	90	79.623(4)	90
V (Å^3)	2358.79(8)	6053.1(2)	1089.56(8)	1729.51(10)
Z	4	8	2	4
μ (mm^{-1})	8.339	7.014	26.798	6.322
D_{calc} (g cm^{-3})	2.527	2.706	2.495	2.303
F(000)	1 696	4 600	780	1 152
Θ Range (°)	2.84–31.99	2.91–32.07	4.18–62.19	3.12–32.41
Index ranges	$-12 \le h \le 7$	$-25 \le h \le 26$	$-10 \le h \le 11$	$-15 \le h \le 14$
	$-44 \le k \le 44$	$-16 \le k \le 15$	$-12 \le k \le 12$	$-14 \le k \le 18$
	$-12 \le l \le 14$	$-45 \le l \le 43$	$-11 \le l \le 12$	$-19 \le l \le 19$
R_{int}	0.0314	0.0337	0.0331	0.0261
Reflections measured	18 472	22 321	9282	6230
Independent reflections	7562	9746	3373	2526
Parameters	309	401	300	128
Goodness-of-fit on F^2	0.931	1.007	0.972	0.982
Final R_1, wR_2 ($I > 2\sigma(I)$) (all data)	0.0315, 0.0556	0.0340, 0.0618	0.0290, 0.0619	0.0232, 0.0514
	0.0521, 0.0587	0.0557, 0.0662	0.0421, 0.0673	0.0264, 0.0521
Largest difference peak and hole (e·Å^{-3})	1.025	1.987	0.949	0.757
	−0.587	−1.397	−0.633	−0.432

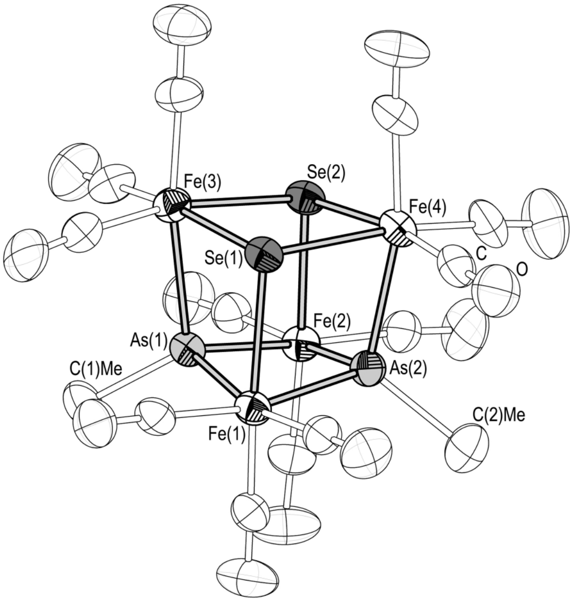

Fig. 1 Molecular structure of the clusters **2** exemplified by **2a** (thermal ellipsoids at 50% probability level). Hydrogen atoms are omitted for clarity. Selected distances (Å) and angles (°) ranges [mean]: **2a**: Fe–Se 2.4569(5)–2.4760(5) [2.4657]; Fe–As 2.3716(5)–2.3949(5) [2.3843]; Fe···Fe 3.676(2)–3.748(1) [3.700]; Se(1)···Se(2) 3.264(1); As(1)···As(2) 2.914(2); Fe–As–Fe 101.44(2)–103.68(2) [102.26]; Fe–Se–Fe 96.60(2)–97.18(2) [96.83]; As–Fe–As 75.12(2), 75.33(2); Se–Fe–Se 82.90(2), 83.17(2); As–Fe–Se 79.40(2)–80.05(2) [79.71]. **2b**: Fe–Te 2.6241(8)–2.6344(8) [2.6274]; Fe–As 2.3955(9)–2.4191(9) [2.4096]; Fe···Fe 3.776(2)–3.959(3) [3.838]; Te(1)···Te(2) 3.458(2); As(1)···As(2) 2.935(3); Fe–As–Fe 102.87(3)–105.22(3) [104.38]; Fe–Te–Fe 93.07(3)–97.82(2) [94.83]; As–Fe–As 74.76(3), 75.08(3); Te–Fe–Te 82.22(2), 82.29(2); As–Fe–Te 79.31(3)–79.88(3) [79.62].

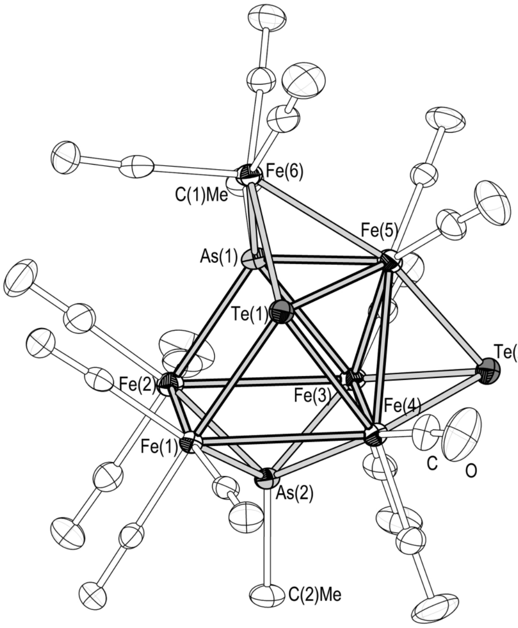

Fig. 2 Molecular structure of the cluster **3b** in the crystal (thermal ellipsoids at 50% probability level). Hydrogen atoms are omitted for clarity. Selected bond distances (Å): Fe(1)–Fe(2) 2.9552(8); Fe(2)–Fe(3) 2.8754(9); Fe(3)–Fe(4) 2.7839(8); Fe(1)–Fe(4) 2.9238(8); Fe(4)–Fe(5) 2.8154(8); Fe(5)–Fe(6) 2.6725(8); Fe(3)–Fe(5) 2.7673(9); Te(1)–Fe(1) 2.6149(6); Te(1)–Fe(4) 2.7089(6); Te(1)–Fe(5) 2.6330(6); Te(1)–Fe(6) 2.5092(6); Te(2)–Fe(3) 2.4537(8); Te(2)–Fe(4) 2.4595(6); Te(2)–Fe(5) 2.4304(6); As(1)–Fe(2) 2.4273(7); As(1)–Fe(3) 2.5311(7); As(1)–Fe(5) 2.4724(8); As(1)–Fe(6) 2.3376(7); As(2)–Fe(1) 2.3063(7); As(2)–Fe(2) 2.3085(7); As(2)–Fe(3) 2.3541(7); As(2)–Fe(4) 2.3543(6).

at the Q atoms, thus making the Fe_2As_2 fragment in the molecules of **2** very distorted from regular cubic geometry.

The more complex molecules of $[Fe_6(\mu_4\text{-}AsMe)_2(\mu_3\text{-}Te)(\mu_4\text{-}Te)(CO)_{15}]$ (**3b**) have exactly double the composition of heavy elements in the cluster core with respect to the initial cluster (Fig. 2), and thus may be considered as the result of a dimerization of the initial cluster molecules with the loss of three CO ligands. The core of the heavy elements can be considered as a tricapped square antiprism without one vertex (with the atoms Fe1 to Fe4, As1, Fe5, and Te1 forming the incomplete antiprism and the atoms Fe6, Te2, and As2 being the caps). Considering each of the Te and AsMe ligands to give $4e^-$ to the cluster, the overall electron number will be 94. According to the 18 electron rule, this corresponds to 7 Fe–Fe bonds, *i.e.* all the neighboring Fe atoms are bound. Most of the Fe–Fe bonds lengths lie in the range of 2.67–2.88 Å which is typical for carbonyl clusters. Only two bonds exceed this range (Fe1–Fe4 2.9238(8) and Fe1–Fe2 2.9552(8) Å) and may be considered as the longest Fe–Fe bonds in the chalcogenide iron-carbonyl clusters (comparable bond distances are found in the clusters $[Fe_3(\mu_3\text{-}S)(AuPPh_3)_2(CO)_9]$, 2.867 Å,[17] and $[Fe_4(\mu_4\text{-}PTol)(\mu_4\text{-}PTol(MeCCH)(CO)_{11}]$, 2.868 Å;[18] the larger distance is only found in the simpler complex $[Fe(\eta^3\text{-}C_3H_5)(CO)_3]_2$, 3.093 Å[19]).

The molecules of $[Fe_4(\mu_4\text{-}AsMe)(\mu_4,\eta^2\text{-}SeAsMe)(CO)_{12}]$ (**4**) in the crystal represent a basket-like structure (Fig. 3), which includes a chain of 4 Fe atoms coordinated by two capping moieties: one is a μ_4-AsMe, and the other is the as yet unknown SeAsMe unit, coordinated in a μ_4,η^2 manner. The latter ligand can be viewed as the heavier congener of RNO,[20] RNS,[21] or RPS[22] ligands, for which several complexes are known, where the ligand bridges two–four metal atoms with different coordination modes. Heavier congeners of this type of ligands are rare: to the best of our knowledge the only example is the compound $[Fe_3(\mu_3\text{-}SbMes)(\mu_3\text{-}MesSbSe)(CO)_{10}]$.[10] In the cluster **4** the As1 atom resides in a tetrahedral environment (CSeFe1Fe2), which points to a $3e^-$ donation of this atom and $6e^-$ for the overall ligand μ_4,η^2-SeAsMe. Supposing the μ_4-AsMe ligand to donate $4e^-$ to the cluster core, the overall electron count will be 66, which corresponds to 3 Fe–Fe bonds. Two of them, Fe1–Fe2 and Fe3–Fe4, are of usual length (2.674(1) Å and 2.623(1) Å, correspondingly); the bond Fe2–Fe3 is noticeably longer (2.884(1) Å). This elongation may be caused by the coordinated SeAsMe unit, whose rigidity does not allow the Fe atoms to be closer (a similar situation occurs in the case of the aforementioned cluster $[Fe_4(\mu_4\text{-}PTol)(\mu_4\text{-}PTol(MeCCH)(CO)_{11}]$, where the Fe atoms forming the longest Fe–Fe bond are coordinated by different ends of the P–C(Me)═CH ligand[18]).

The last product of the thermolysis of the Se-containing cluster **1a** characterized by X-ray diffraction does not contain Se: $[Fe_3(\mu_3\text{-}AsMe)_2(CO)_9]$ (**5**). The molecular structure of this compound is typical for $50e^-$ clusters with square-pyramidal core Fe_3EE' (E = element of group 15 or 16) and an Fe atom on the apex

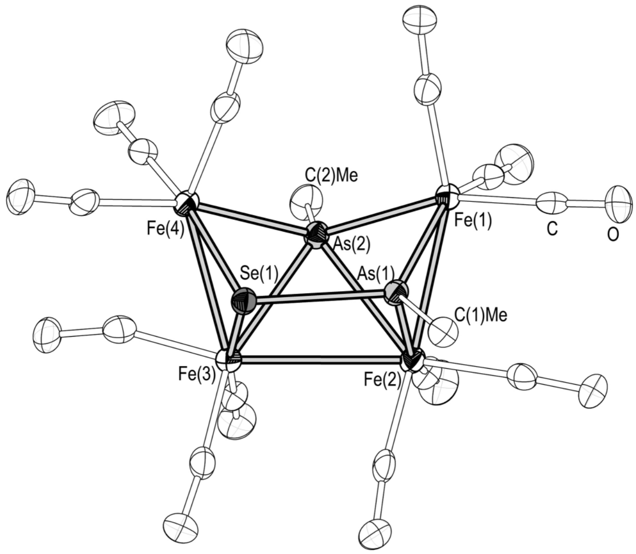

Fig. 3 Molecular structure of the cluster **4** in the crystal (thermal ellipsoids at 50% probability level). Hydrogen atoms are omitted for clarity. Selected distances (Å) and angles (°): Fe(1)–Fe(2) 2.6737(10); Fe(2)–Fe(3) 2.8842(10); Fe(3)–Fe(4) 2.6232(10); Fe(1)–As(1) 2.2922(9); Fe(2)–As(1) 2.3153(9); Fe(1)–As(2) 2.3685(9); Fe(2)–As(2) 2.5199(8); Fe(3)–As(2) 2.4749(9); Fe(4)–As(2) 2.4477(8); Fe(3)–Se(1) 2.4072(9); Fe(4)–Se(1) 2.3772(8); As(1)–Se(1) 2.4042(7); Fe(1)–As(1)–Fe(2) 70.94(3); Fe(1)–As(1)–Se(1) 118.08(3); Fe(2)–As(1)–Se(1) 101.25(3); Fe(4)–Se(1)–As(1) 104.99(3); Fe(3)–Se(1)–Fe(4) 66.50(3); As(1)–Se(1)–Fe(3) 90.35(3).

(Fig. 4). Among the clusters with E = E′ = As, there are only two analogs known, $[Fe_3(\mu_3\text{-}AsPh)_2(CO)_9]$,[23] and $[Et_4N]_2[Fe_3(\mu_3\text{-}AsFe(CO)_4)_2(CO)_9]$,[24] which reveal almost the same geometrical parameters of the cluster core. The only difference is that all the corresponding bond lengths are smaller in cluster **5**, possibly owing to the poorer donating effect of the Me groups as compared to that of Ph units. In the crystal structure of **5** the iron atoms as well as three carbonyl ligands lie in the mirror plane. The As···As distance (2.7980(3) Å) is smaller than the sum of the van der Waals radii, which is typical for such types of clusters.[25]

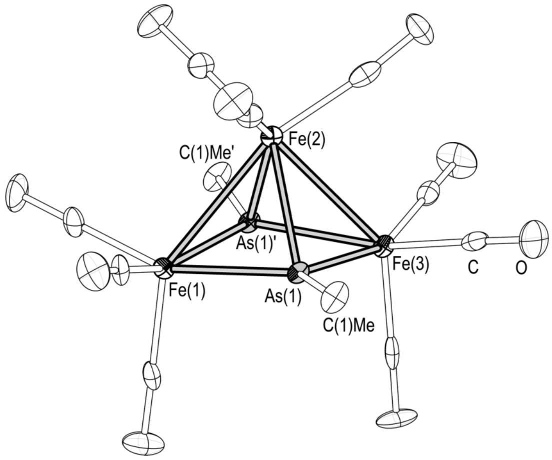

Fig. 4 Molecular structure of the cluster **5** in the crystal (thermal ellipsoids at 50% probability level; dashed atoms are mirror plane equivalents). Hydrogen atoms are omitted for clarity. Selected distances (Å) and angles (°): Fe(1)–Fe(2) 2.7346(9); Fe(2)–Fe(3) 2.7401(8); As(1)–Fe(1) 2.3175(5); As(1)–Fe(2) 2.3311(5); As(1)–Fe(3) 2.3124(5); As(1)–As(1)′ 2.7980(3); Fe(1)–As(1)–Fe(3) 105.04(2); As(1)–Fe(1)–As(1)′ 74.27(2); Fe(1)–Fe(2)–Fe(3) 84.31(2); As(1)–Fe(2)–As(1)′ 73.76(2); As(1)–Fe(3)–As(1)′ 74.46(2).

The reactions involving Se clusters led to lower yields of the main products, as compared to the Te clusters, along with the formation of noticeable amounts of by-products. Thus, the Se-containing clusters were not characterized so extensively as their Te analogs. Moreover, the compound **2a** could not be fully separated from the starting cluster **1a** due to similar solubility and chromatographic behaviour. Thus, its IR and mass spectra, as well as elemental analysis, could not be properly performed. Nevertheless, having the spectra of the Te-containing clusters for reference, the NMR spectra of corresponding pairs (**2a** and **2b**, **3a** and **3b**) reveal practically the same signals both for ^1H and ^{13}C experiments. Analogously, the IR spectra in the ν_{CO} region contain practically the same pattern for each pair of compounds (weaker signals for **2a** are hidden by the stronger ones of **1a** impurities), with the shift of the ν_{CO} bands to higher frequencies for Se-containing analogs, according to the donor abilities of the chalcogen atoms. On the basis of spectroscopic data we suppose that the cluster **3a**, for which the X-ray crystal structure could not be determined, is isostructural to its Te analog **3b**. The IR spectra of **2** do not resemble those of the known cubane clusters $[Co_4Sb_4(CO)_{12}]$,[26] $[Fe_4(SbFeCp(CO)_2)_4(CO)_{12}]$,[7] $[Fe_4Q_4(CO)_{12}]$ (Q = S, Se,[3] Te[4]), and $[Fe_4(AsMe)_4(CO)_{12}]$,[9] evidently, because of the lower symmetry of the cluster core. For all the compounds the signals of the As–Me protons in ^1H NMR spectra are shifted to the lower field (1.74–2.68 ppm) in comparison with mononuclear carbonyl species of coordinated $MeAsH_2$ (about 0.5 ppm), which supports the coordination of the AsMe ligand to several metal atoms (analogously to the aforementioned cluster $[Fe_4(AsMe)_4(CO)_{12}]$).[9]

Reaction pathways

According to the structure of the clusters **3**, whose cluster core contains exactly double the number of heavy atoms as compared with **1**, we suppose that they form as a result of dimerization of the starting clusters **1**. This assumption is supported by the fact that the compounds **3** are the main products in the reaction mixture, if the acetonitrile reaction solution is not heated too long. Prolonged heating leads to disappearance of both products **2** and **3**, owing to decomposition. Consequently, we suppose the cubane clusters **2** to be the result of release of two iron-carbonyl vertices from the clusters **3** (Scheme 2). To prove this, samples of pure clusters **3** were heated in acetonitrile solution. After 3 h of heating at 90 °C (the conditions close to those during the initial thermolysis), the compound **3** was consumed, while the corresponding cubane **2** appeared as the main component of the solution, according to the characteristic signals in IR spectra. Hence, the conversion of **1** into **2** with the intermediate formation of **3** is the main reaction pathway.

$$\mathbf{1} \xrightarrow[\text{2x, −3CO}]{\text{MeCN, }\Delta} \mathbf{3} \xrightarrow[-2\{Fe(CO)_x\}]{\Delta} \mathbf{2}$$

Scheme 2

This result is in contrast with the formerly discovered transformation route of the $[Fe_3Q_2(CO)_9]$ clusters, which were found to lose one $Fe(CO)_3$ vertex and to transform into the corresponding $[Fe_2Q_2(CO)_6]$ species upon treatment with polar reagents, such as CH_3CN, or NaOMe in methanol.[16] The di-iron species can further dimerize to corresponding cubanes $[Fe_4Q_4(CO)_{12}]$, either by thermal (for Q = Te) or photochemical (for Q = S) activation. Thus, the conversion of Fe_3Q_2 into Fe_4Q_4 clusters goes primarily according to the dissociative pathway. A similar discrepancy in the behaviour of the clusters $[Fe_3Q(AsMe)(CO)_9]$ *versus* $[Fe_3Q_2(CO)_9]$ is mentioned in the literature,[14] on the basis of their reactions with complexes $[(PPh_3)_2Pt(C_2Ph_2)]$ and $[Cp_2Cr_2(\mu\text{-}S)(\mu\text{-}SCMe_3)_2]$, as well as on the thermogravimetric data. In all the reactions the mixed Q/As clusters are found to be more inert than their chalcogenide-only analogs. This difference in reactivity of the Fe_3Q_2 and $Fe_3Q(AsMe)$ clusters may be explained by stronger binding of metal atoms in the cluster by the μ_3-AsMe ligand as compared to the μ_3-Q unit. It also formally explains the formation of by-products **4** and **5** during the thermolysis of **1a**. Each of these two compounds contains two μ_3-AsMe units in the molecule. Therefore, supposing them to be the products of consecutive degradation of **3a**, the loss of one (for **4**) and two (for **5**) Se atoms is observed, but not that of the AsMe groups, which still remain in both compounds. Unfortunately, the small amounts of these clusters obtained from the reaction mixtures were not sufficient for further experiments to prove this hypothesis.

Considering the first step of the associative pathway, namely the fusion of two cluster molecules into a bigger one, similar reactions (but no dimerizations) are known for both $[Fe_3Q(ER)(CO)_9]$ (E = group 15 element) and $[Fe_3Q_2(CO)_9]$ clusters. In fact, the clusters with the square-pyramidal core Fe_3Q_2 are known to form octahedral derivatives $Fe_3(ML_n)Q_2$ in reactions with the sources of coordinatively unsaturated species (such as $Pt(PPh_3)_4$, $Pd(PPh_3)_4$,[27] $Ru(CO)_4(C_2H_4)$[28]). Analogous behaviour was observed in the reactions of $[Fe_3S(PR)(CO)_8(CRR')]$ with $[Fe_2(CO)_9]$[15] and of $[Fe_3Q(AsMe)(CO)_9]$ with $[Cp^*M(CO)_2]$ (M = Rh, Ir).[13] Clusters with the core Fe_3QQ' (with all combinations of Q, Q′ = S, Se, Te, except QQ′ = S_2) react with binuclear complex $[CpMo(CO)_3]_2$ to form insertion products containing the whole Mo_2 fragment in the cluster core. However, the final products contain only 2 Fe atoms (one Fe atom fewer), $[Cp_2Mo_2Fe_2(CO)_nQQ']$ (n = 6–8 depending on the chalcogen atom combination[29]). Identical behaviour is known for the cluster $[Fe_3Se(AsMe)(CO)_9]$, which in the reaction with $[CpMo(CO)_3]_2$ gives a derivative $[Cp_2Mo_2Fe_2(CO)_7Q(AsMe)]$ as the main product.[12] Thus, one may consider the merging of two cluster cores as a process similar to the addition of complex species to the cluster core known before for the species of lower nuclearity. Interestingly, similar dimerization processes are not known for the chalcogenide-only clusters $[Fe_3Q_2(CO)_9]$. The reason is, probably, in the greater rates of dissociative processes, rather than those of association and merging, especially for reactions in dilute solutions. The latter is usually known for heavy polynuclear clusters.

It is interesting to note that all mentioned addition reactions of either mono- or bimetallic complexes to clusters of types Fe_3Q_2 and $Fe_3Q(AsMe)$ were carried out upon heating in non-polar media, such as hexane or toluene. In contrast, no changes but slight decomposition of **1** are observed upon heating in toluene for several hours at 110 °C. Hence, the acetonitrile solvent must be necessary for the formation of **3**, in spite of the fact that polar media favour the dissociation processes. Apparently, the role of acetonitrile is the activation of the cluster molecules by weakening the metal–metal bonds, which leads to a more open cluster core, capable of merging with another cluster molecule. Such reactions are well documented for the cluster $[Fe_3Te_2(CO)_9]$, the interaction with Lewis bases (L) leads to products of ligand addition, $[(CO)_6Fe_2Te_2(Fe(CO)_3L)]$ (L = PR_3, NR_3, CO, Bu^tNC).[30] Analogous addition products are not typical for $[Fe_3Se_2(CO)_9]$. It was established that the greater the electronegativity of the Q atoms in such clusters, the lower is the probability of ligand addition with respect to dissociative processes.[31] Considering the same principle to be correct for the clusters with both Q and AsMe ligands, the dissociation with the loss of CO groups should be more typical for the transformation of Se-containing clusters **1a** than for Te analogs **1b**, which seems to be the reason for lower yields and larger amounts of by-products obtained for Se clusters.

Conclusions

The first examples of cubane-type iron clusters $[Fe_4Q_2(AsMe)_2(CO)_{12}]$, which simultaneously contain elements of groups 15 and 16 in the cluster core, have been synthesized by thermolysis of $[Fe_3Q(AsMe)(CO)_9]$ in acetonitrile, and structurally characterized. It was shown that the reaction proceeds by a so far unknown route, which includes the formation of the clusters $[Fe_6Q_2(AsMe)_2(CO)_{15}]$, as the result of dimerization of the starting compounds. This pathway can be designated as “associative”, in contrast to the formerly known “dissociative” routes known for the analogous chalcogen-only tri-iron clusters $[Fe_3Q_2(CO)_9]$, which show a tendency to lose one iron vertex upon heating in polar solvents. The stronger binding of the As vertex to the cluster core is considered to be one reason for the associative behaviour, and the structures of the reaction by-products confirm this thesis. It was shown that the use of a polar solvent is necessary for the reaction, but it does not proceed in the presence of high CO pressures, unlike the case of $[Fe_3Q_2(CO)_9]$ clusters. The method might open a way towards heterocubane clusters with the mixed 15/16 group element $[Fe_4Q_2(ER)_2]$ core, starting from the various known tri-iron clusters $[Fe_3Q(ER)(CO)_9]$.

Experimental

General procedures

All operations were carried out under inert atmospheres of nitrogen or argon. The starting reagents, **1a** and **1b** were prepared according to known methods.[11,12] Solvents were distilled in inert atmospheres over common drying agents; silica gel for column chromatography (Merck Ceduran Si 60, 0.063–0.200 mm) was activated by heating in vacuum at 180 °C for 3 days. The IR spectra were recorded on a Varian FTS 800 spectrometer, for the solutions in hexane. The NMR spectra were recorded on a Bruker Avance 400 spectrometer (^{1}H: 400.132 MHz, ^{13}C: 100.627 MHz), for the solutions in CD_2Cl_2. Chemical shifts (δ, ppm) were referenced to the signals of the solvent (^{1}H and ^{13}C spectra, δ_H = 5.32 ppm, δ_C = 53.90 ppm). Mass spectra were measured on a Finnigan ThermoQuest TSQ 7000 spectrometer (ESI for solutions in CH_2Cl_2/MeOH mixtures with addition of 10 mmol l^{-1} NH_4OAc, negative region, or FI/FD).

Syntheses of $[Fe_4(\mu_3\text{-}Q)_2(\mu_3\text{-}AsMe)_2(CO)_{12}]$ (Q = Se (2a), Te (2b)), $[Fe_6(\mu_4\text{-}AsMe)_2(\mu_3\text{-}Q)(\mu_4\text{-}Q)(CO)_{15}]$ (Q = Se (3a), Te (3b)), $[Fe_4(\mu_4\text{-}AsMe)(\mu_4,\eta^2\text{-}TeAsMe)(CO)_{12}]$ (4), and $[Fe_3(\mu_3\text{-}AsMe)_2(CO)_9]$ (5)

In a typical experiment the starting compound **1a** (0.200 g, 0.340 mmol), or **1b** (0.200 g, 0.314 mmol) was placed in an ampoule with a Teflon stopcock. About 10 ml of CH_3CN were added, the vessel was shortly evacuated and placed in an oil bath (90 °C) for 2 days. The resulting dark olive-green mixture was evaporated to dryness; the residue was extracted with toluene (*ca.* 20 ml). A small amount of silica gel was added to the extract and the mixture was dried under vacuum. Chromatography on a silica column (2 × 20 cm) gave the following fractions:

(1) (hexane) purple band, little amounts of $[Fe_3Q_2(CO)_9]$ (proven on the basis of IR spectra and TLC);

(2) (hexane) orange-brown band, a mixture of the initial cluster **1** (*ca.* 20%) and the product **2**;

(3) (hexane–toluene 9/1 v/v) dark grey-brown band, contains the product **3** (in the case of Se clusters it also contains an amount of unidentified compounds, which can be further separated by TLC).

The second fraction was concentrated to a small volume and cooled, to give the mixture of **1** and **2** as a dark-brown crystalline powder. The mixture was washed several times with 3 ml portions of hexane to remove the cluster **1**; the cluster **2** is only poorly soluble in hexane and may be further recrystallized from CH_2Cl_2. The third fraction was concentrated under vacuum to *ca.* 2 ml and cooled overnight at 0 °C. The obtained fine crystalline powder of **3** was filtered, dried, and recrystallized from CH_2Cl_2. Compound **5** was obtained from a minor fraction (found only in the case of the Se-containing cluster) coming just before the third one. This orange–brown fraction was evaporated to dryness, redissolved in *ca.* 1 ml of CH_2Cl_2, and kept at −25 °C; a crop of dark-red cubic crystals of **5** formed in a few days. Compound **4** was obtained as a few plate-like dark crystals from the tails of the third fraction, collected separately, by concentrating to a volume of *ca.* 1 ml and refrigerating. Crystals of **4** are insoluble in toluene. Yields (% with the deduction of the starting clusters **1**, recovered after the reaction): **2a** (0.017 g, 14%); **2b** (0.030 g, 24%); **3a** (0.027 g, 18%); **3b** (0.043 g, 29%); **4** (a few crystals); **5** (0.010 g, 12% based on As).

Compound 2a. IR ν_{max}/cm^{-1} 2044 s (CO); δ_H 1.74 (s, CH_3); δ_C 205.0, 203.5, 201.2, 199.7 (intensities ratio 2 : 1 : 1 : 2, all s, CO), 15.37 (s, CH_3).

Compound 2b. Anal. Found: C, 16.7; H, 0.77; Calc. for $C_{15}H_8As_2Cl_2Fe_4O_{12}Te_2$ (*i.e.* for the solvate **2b**·CH_2Cl_2): C, 16.7; H, 0.75%; IR ν_{max}/cm^{-1} 2040 s, 2000 m, 1992 m, 1987 m (CO); δ_H 1.79 (s, CH_3); δ_C 205.0, 203.5, 201.3, 199.8 (intensities ratio 2 : 1 : 1 : 2, all s, CO), 15.42 (s, CH_3); *m*/*z* (FI/FD) 995.8 [M^+].

Compound 3a. IR ν_{max}/cm^{-1} 2075 m, 2037 s, 2027 s, 2010 m, 1998 m, 1989 w, 1980 w (CO); δ_H 2.24 (s, CH_3); δ_C 210.1, 208.3, 205.2, 203.7 (all s, CO), 25.1 (s, CH_3); *m*/*z* (FI/FD) 1093.6 [M^+].

Compound 3b. Anal. Found: C, 17.8; H, 0.97; Calc. for $C_{17.5}H_7As_2ClFe_6O_{15}Te_2$ (*i.e.* for the solvate **3b**·0.5CH_2Cl_2): C, 17.1; H, 0.57%; IR ν_{max}/cm^{-1} 2070 m, 2034 s, 2027 s, 2023 s, 2005 m, 1993 m, 1987 w, 1973 w (CO); δ_H 2.68, 2.50 (both s, CH_3); δ_C 209.9, 209.7, 208.9, 207.9, 207.3, 207.2 (all s, CO), 29.4 (s, CH_3); *m*/*z* (ESI) 970.4 (100, M – 2Fe – 6CO + AcO^-), 998.4 (30, M – 2Fe – 5CO + AcO^-).

Compound 5. IR ν_{max}/cm^{-1} 2038 s, 2016 s, 1997 s (CO); δ_H 2.59 (s, CH_3); δ_C 215.0 (s, CO), 11.7 (s, CH_3); *m*/*z* (ESI) 658.8 (100, M + AcO^-), 630.7 (55, M – CO + AcO^-), 598.7 (7, M^-), 574.7 (15, M – 3CO + AcO^-).

Heating of cluster 1a in acetonitrile under CO pressure

A sample of **1a** (0.357 g, 0.607 mmol) was placed in a 150 ml autoclave, 20 ml of acetonitrile were added, the autoclave was purged 3 times with 50 bar N_2, filled with 90 bar CO, and placed in a rotating oven. After 36 h of heating at 90 °C the autoclave was opened and vented, the clear wine-red solution was transferred in a flask in N_2 atmosphere (no traces of decomposition were found). Shortly afterwards small dark crystals started to precipitate at the bottom of the flask. According to the IR spectra, the solution contained only the starting cluster **1a**, and the crystals have been identified as the same compound.

Treatment of the clusters 1a, 1b with NaOMe in methanol

Analogous to the published procedures,[16,28] cluster **1a** or **1b** (*ca.* 0.20 mmol) was added to methanol solution of KOMe (obtained from 0.066 g (1.7 mmol) of K and 20 ml of MeOH). The mixture was stirred for 1 h. The resulting clear solution was diluted with 20 ml of hexane and 20 ml of water, and acidified with 0.5 ml of 5 M HCl. The organic layer was collected, the aqueous phase was washed with another 20 ml portion of hexane, leaving an almost colorless solution. The combined hexane fraction was washed with water and dried over $MgSO_4$. This solution contained only starting cluster **1**, according to IR spectra and TLC.

Conversion of the clusters 3a,b into 2a,b in acetonitrile

A sample of 0.015 g of **3** (*ca.* 0.013 mmol) was placed in a tube with a Teflon stopcock. 2 ml of acetonitrile were added, the vessel was closed and heated at 80 °C for 3 h. After cooling, a number of small crystals formed on the bottom of the vessel, which were shown to be the cubane clusters **2**, according to IR spectra in hexane. About 1 ml of the acetonitrile solution was evaporated to dryness, the rest was redissolved in CH_2Cl_2 and analysed by TLC and IR. The TLC contains mostly the spot of compound **2** (compared with the pure sample) and only other weak spots. The IR spectra, being quite noisy, still resembled all the features of the spectra of **2** (sharp bands at *ca.* 2040 cm^{-1} and broad one at 1990 cm^{-1}) and contained no bands characteristic of **1** or **3**.

X-ray data collection

Crystals of the compounds **2a**, **2b**·CH_2Cl_2, **3b**·0.5CH_2Cl_2 and **4** were used for data collection on a Oxford Diffraction Gemini Ultra diffractometer with CCD detector and multilayer mirror optics for CuK_α radiation or graphite monochromator for MoK_α radiation. The X-ray structure analysis for **2a**·CH_2Cl_2, **2b^m** and **2b^o** was carried out on a Stoe IPDS I diffractometer with AgK_α radiation. The structures were solved by direct methods (SIR-97[32]) and refined by full-matrix least squares on F^2 (SHELXL-97[33]). The H atoms were calculated geometrically and a riding model was applied during the refinement process. Due to disordering of the solvent molecule CH_2Cl_2 in **2a**·CH_2Cl_2 the final *R* values are slightly higher than usual. Compound **2b**^{o} crystallizes in an acentric space group, probably as an inversion twin, for which the Flack parameter of 0.51(2) was found after refinement. Large residual density in **2b** gave a hint towards the presence of a second orientation of the cluster. This minor component turned out to be only about four percent occupied. Thus only the minor positions of tellurium atoms could be located and were refined isotropically.

Acknowledgements

This work was supported by the Deutsche Forschungsgemeinschaft and the Fonds der Chemischen Industrie, as well as a Russian Federation President grant (financial support for NAP, project MK-4130.2009.3), Russian Foundation of Basic Research grant no. 10-03-00385, and state contract no. 02.740.11.0628.

Notes and references

1 (*a*) P. Venkateswara Rao and R. H. Holm, *Chem. Rev.*, 2004, **104**, 527–560; (*b*) S. Groysman and R. H. Holm, *Biochemistry*, 2009, **48**, 2310–2320.

2 (*a*) C. R. Sharp, J. S. Duncan and S. C. Lee, *Inorg. Chem.*, 2010, **49**, 6697–6705; (*b*) C. Zhou and R. H. Holm, *Inorg. Chem.*, 1997, **36**, 4066–4077; (*c*) T. Trinh, B. K. Teo, J. A. Ferguson, T. J. Meyer and L. F. Dahl, *J. Am. Chem. Soc.*, 1977, **99**, 408–416; (*d*) H. Ogino, H. Tobita, K. Yanagisawa, M. Shimoi and C. Kabuto, *J. Am. Chem. Soc.*, 1987, **109**, 5847–5848.

3 L. L. Nelson, F. Y.-K. Lo, A. David Rae and L. F. Dahl, *J. Organomet. Chem.*, 1982, **225**, 309–329.

4 L. E. Bogan, D. A. Lesch and T. B. Rauchfuss, *J. Organomet. Chem.*, 1983, **250**, 429–438.

5 (*a*) J. S. Duncan, T. M. Nazif, A. K. Verma and S. C. Lee, *Inorg. Chem.*, 2003, **42**, 1211–1224; (*b*) A. K. Verma, T. N. Nazif, C. Achim and S. C. Lee, *J. Am. Chem. Soc.*, 2000, **122**, 11013–11014; (*c*) H. Link, A. Decker and D. Fenske, *Z. Anorg. Allg. Chem.*, 2000, **626**, 1567–1574; (*d*) U. Riese, K. Harms, J. Pebler and K. Dehnicke, *Z. Anorg. Allg. Chem.*, 1999, **625**, 746–754.

6 E. Röttinger and H. Vahrenkamp, *Angew. Chem., Int. Ed. Engl.*, 1978, **17**, 273–274.

7 S. N. Konchenko, A. V. Virovets, S. A. Apenina and S. V. Tkachev, *Inorg. Chem. Commun.*, 1999, **2**, 555–557.

8 See for example: (*a*) R. H. Holm and C. Richard, in *Advances in Inorganic Chemistry*, Academic Press, 1992, vol. 38, pp. 1–71; (*b*) T. A. Scott and R. H. Holm, *Inorg. Chem.*, 2008, **47**, 3426–3432; (*c*) J. Sun, C. Tessier and R. H. Holm, *Inorg. Chem.*, 2007, **46**, 2691–2699; (*d*) M. Koutmos, I. P. Georgakaki, P. Tsiolis and D. Coucouvanis, *Z. Anorg. Allg. Chem.*, 2008, **634**, 255–261; (*e*) M. Koutmos, I. P. Georgakaki and D. Coucouvanis, *Inorg. Chem.*, 2006, **45**, 3648–3656; (*f*) M. Harmjanz, W. Saak, D. Haase and S. Pohl, *Chem. Commun.*, 1997, 951–952; (*g*) T. Komuro, H. Kawaguchi, J. Lang, T. Nagasawa and K. Tatsumi, *J. Organomet. Chem.*, 2007, **692**, 1–9; (*h*) H. Kawaguchi, K. Yamada, S. Ohnishi and K. Tatsumi, *J. Am. Chem. Soc.*, 1997, **119**, 10871–10872; (*i*) S. Inomata, K. Hiyama, H. Tobita and H. Ogino, *Inorg. Chem.*, 1994, **33**, 5337–5342; (*j*) S. E. Nefedov, I. L. Eremenko, A. A. Pasynskii, A. I. Yanovsky and Y. T. Struchkov, *Russ. J. Inorg. Chem. (Transl. of Zh. Neorg. Khim.)*, 1992, **37**, 2712; (*k*) B. Bechlars, I. Issac, R. Feuerhake, R. Clérac, O. Fuhr and D. Fenske, *Eur. J. Inorg. Chem.*, 2008, 1632–1644.

9 E. Röttinger and H. Vahrenkamp, *J. Organomet. Chem.*, 1981, **213**, 1–9.

10 S. N. Konchenko, N. A. Pushkarevsky and M. Scheer, *J. Organomet. Chem.*, 2002, **658**, 204–209.

11 S. N. Konchenko, N. A. Pushkarevsky, A. V. Virovets and M. Scheer, *Dalton Trans.*, 2003, 581–585.

12 S. N. Konchenko, A. V. Virovets, P. A. Petrov and S. V. Tkachev, *Russ. Chem. Bull.*, 1999, **48**, 988–990.

13 N. A. Pushkarevsky, D. A. Bashirov, A. V. Litke, A. V. Virovets, N. V. Kurat'eva, M. Scheer and S. N. Konchenko, *Russ. J. Coord. Chem.*, 2008, **34**, 871–883.

14 A. A. Pasynskii, S. S. Shapovalov, Z. V. Dobrokhotova, K. A. Lysenko, S. N. Konchenko and N. A. Pushkarevsky, *Russ. J. Coord. Chem.*, 2009, **35**, 112–119.

15 B. Eber, G. Huttner, D. Günauer, W. Imhof and L. Zsolnai, *J. Organomet. Chem.*, 1991, **414**, 361–371.

16 P. Mathur, D. Chakrabarty and M. M. Hossain, *J. Organomet. Chem.*, 1991, **401**, 167–172.

17 E. Roland, K. Fischer and H. Vahrenkamp, *Angew. Chem., Int. Ed. Engl.*, 1983, **22**, 326–327.

18 J. T. Jaeger, A. K. Powell and H. Vahrenkamp, *Chem. Ber.*, 1988, **121**, 1729–1738.

19 C. F. Putnik, J. J. Welter, G. D. Stucky, M. J. D'Aniello Jr., B. A. Sosinsky, J. F. Kirner and E. L. Muetterties, *J. Am. Chem. Soc.*, 1978, **100**, 4107–4116.

20 (*a*) G. Gervasio, R. Rossetti and P. L. Stanghellini, *J. Chem. Soc., Chem. Commun.*, 1977, 387–388; (*b*) M. J. Barrow and O. S. Mills, *J. Chem. Soc. A*, 1971, 864–868; (*c*) K. K. H. Lee and W. T. Wong, *J. Chem. Soc., Dalton Trans.*, 1996, 3911–3912.

21 (*a*) R. Meij, D. J. Stufkens, K. Vrieze, A. M. F. Brouwers, J. D. Schagen, J. J. Zwinselman, A. R. Overbeek and C. H. Stam, *J. Organomet. Chem.*, 1979, **170**, 337–354; (*b*) W.-Y. Yeh, C. Stern and D. F. Schriver, *Inorg. Chem.*, 1996, **35**, 7857–7862; (*c*) M. Herberhold and W. Bühlmeyer, *Angew. Chem., Int. Ed. Engl.*, 1984, **23**, 80–81.

22 (*a*) H. Alper, F. W. B. Einstein, J. F. Petrignani and A. C. Willis, *Organometallics*, 1983, **2**, 1422–1426; (*b*) Z. Weng, W. K. Leong, J. J. Vittal and L. Y. Goh, *Organometallics*, 2003, **22**, 1645–1656; (*c*) R. M. De Silva, M. J. Mays, P. R. Raithby and G. A. Solan, *J. Organomet. Chem.*, 2002, **642**, 237–245.

23 M. Jacob and E. Weiss, *J. Organomet. Chem.*, 1977, **131**, 263–271.

24 R. E. Bachman, S. K. Miller and K. H. Whitmire, *Organometallics*, 1995, **14**, 796–803.

25 G. Gervasio, *J. Organomet. Chem.*, 1993, **445**, 147–155.

26 A. S. Foust and L. F. Dahl, *J. Am. Chem. Soc.*, 1970, **92**, 7337–7341.

27 P. Mathur, D. Chakrabarty, M. M. Hossain and R. S. Rashid, *J. Organomet. Chem.*, 1991, **420**, 79–86.

28 P. Mathur, D. Chakrabarty and M. M. Hossain, *J. Organomet. Chem.*, 1991, **418**, 415–420.

29 (*a*) P. Mathur, M. M. Hossain, S. B. Umbarkar, C. V. V. Satyanarayana, A. L. Rheingold, L. M. Liable Sands and G. P. A. Yap, *Organometallics*, 1996, **15**, 1898–1904; (*b*) P. Mathur, S. Ghose, M. M. Hossain, C. V. V. Satyanarayana and M. F. Mahon, *J. Organomet. Chem.*, 1997, **543**, 189–199; (*c*) L. E. Bogan, T. B. Rauchfuss and A. L. Rheingold, *J. Am. Chem. Soc.*, 1985, **107**, 3843–3850; (*d*) P. Mathur, M. M. Hossain and A. L. Rheingold, *Organometallics*, 1994, **13**, 3909–3913.

30 D. A. Lesch and T. B. Rauchfuss, *Organometallics*, 1982, **1**, 499–506.

31 R. Rossetti, P. L. Stanghellini, O. Gambino and G. Cetini, *Inorg. Chim. Acta*, 1972, **6**, 205–210.

32 A. Altomare, M. C. Burla, M. Camalli, G. L. Cascarano,C. Giacovazzo, A. Guagliardi, A. G. G. Moliterni, G. Polidori and R. Spagna, *J. Appl. Crystallogr.*, 1999, **32**, 115–119.

33 G. M. Sheldrick, *Acta Crystallogr., Sect. A: Found. Crystallogr.*, 2008, **64**, 112–122.